HHS Public Access

Author manuscript

Exp Biol Med (Maywood). Author manuscript; available in PMC 2016 March 01.

Published in final edited form as:

Exp Biol Med (Maywood). 2015 March ; 240(3): 361–374. doi:10.1177/1535370214561586.

Structural Insights into the Functional Versatility of WWOX Tumor Suppressor

Amjad Farooq[*]

Department of Biochemistry & Molecular Biology, Leonard Miller School of Medicine, University of Miami, Miami, FL 33136

Abstract

Recent work on WWOX tumor suppressor is beginning to shed new light on both the molecular mechanism of action of its WW domains as well as the contiguous catalytic domain. Herein, the structural basis underlying the ability of WW1 domain to bind to various physiological ligands and how the orphan WW2 tandem partner synergizes its ligand binding in the context of WW1-WW2 tandem module of WWOX is discussed. Notably, the WW domains within the WW1-WW2 tandem module physically associate so as to adopt a fixed spatial orientation relative to each other. In this manner, the association of WW2 domain with WW1 hinders ligand binding to the latter. Consequently, ligand binding to WW1 domain not only results in the displacement of WW2 lid but also disrupts the fixed orientation of WW domains in the liganded conformation. Equally importantly, structure-guided functional approach suggests that the catalytic domain of WWOX likely serves as a retinal oxidoreductase that catalyzes the reversible oxidation and reduction of all-trans-retinal. Collectively, this review provides structural insights into the functional versatility of a key signaling protein with important implications on its biology.

Keywords

WW-ligand interactions; Allosteric communication; Retinal oxidoreductase; Retinoid metabolism

Introduction

The modular architecture of WWOX tumor suppressor, comprised of a tandem copy of WW domains (designated WW1 and WW2) located N-terminal to the short-chain dehydrogenase/reductase (SDR) domain, exquisitely befits its role as a key player in mediating a multitude of cellular activities including growth, proliferation, apoptosis and tumor suppression (1–4). In particular, aberrant expression of WWOX is believed to be linked to the progression of many forms of cancer, including those of breast and prostate (5–12). Notably, the ability of WWOX to drive normal and aberrant cellular signaling is largely dependent upon the ability of its WW1 domain to recognize PPXY motifs located within cognate ligands such as WBP1/2 signaling adaptors (13, 14), ErbB4 receptor kinase (15), p73 tumor suppressor (16) as well as many others (17).

[*]To whom correspondence should be addressed: amjad@farooqlab.net | tel 305-243-2429 | fax 305-243-3955.

It is telling that these aforementioned ligands of WWOX are also cellular targets of WW domains of YAP transcriptional regulator—a key player driving the Hippo signaling cascade involved in regulating the size of organs and in the suppression of tumors through inhibiting cellular proliferation and promoting apoptosis (18–22). In addition to WBP1/2 (23, 24), ErbB4 (25, 26) and p73 (27), YAP is also known to interact with a wide variety of other cellular proteins such as TMG2 transmembrane protein (28), PTPN14 phosphatase (29), SMAD7 signaling adaptor (30) and PTCH1 transmembrane receptor (31). Importantly, it is believed that WWOX antagonizes the transactivation function of YAP by virtue of its ability to competitively bind to these proteins and, in so doing, plays a central role in the maintenance of cellular homeostasis (15, 19).

While WW1 domain of WWOX is critical to its ability to recognize putative PPXY ligands, no physiological ligands of the WW2 domain have hitherto been identified. Interestingly, previous studies have suggested that the WW2 domain not only structurally stabilizes the WW1 domain within the context of WW1-WW2 tandem module but that it also augments ligand binding to WWOX (14, 32). This earlier work suggested that the WW2 domain is an orphan domain whose primary physiological role is to chaperone and aid ligand binding to WW1 domain within WWOX. While the role of WW domains of WWOX in cellular signaling is well-characterized, little light has hitherto been shed on the physiological function of the SDR domain. In this review, detailed insights into the structure-function relationships of the WW domains of WWOX are provided. Additionally, on the basis of structure-guided analysis, compelling evidence is provided to postulate that the SDR domain of WWOX serves as a retinal oxidorductase in cellular signaling.

WW2 domain chaperones and aids ligand binding to WW1 domain of WWOX

The notion that WWOX binds to its cellular partners primarily via its WW1 domain first came to prominence via a series of cell-based studies (13, 15–17, 33). However, these studies raised the question as to the physiological role of WW2 domain. The notion that the WW2 domain of WWOX could be an orphan module devoid of ligand binding capability but primarily serves as a chaperone to augment the physiological function of WW1 domain within WWOX was later confirmed using an array of biophysical tools. Firstly, the WW2 domain was shown to possess no intrinsic binding to its putative PPXY ligands derived from WWOX-binding partners WBP1/2 (14) and ErbB4 (32). Secondly, studies also indicated that the WW2 domain augmented the binding of WW1 domain to PPXY ligands between two- to three-folds (14, 32). Thirdly, it was shown that while the orphan WW2 domain displayed high thermal stability and was structurally folded in isolation, the WW1 domain in sharp contrast was partially unstructured alone and only adopted a canonical triple-stranded β-fold only in the context of WW1-WW2 tandem module (14).

The above-mentioned findings imply that the WW2 domain serves as a chaperone that not only aids ligand binding but also promotes the folding of WW1 domain within the context of the WW1-WW2 tandem module of WWOX. That this is likely to be a rule rather than an isolated case is further confirmed by our recent biophysical analysis and comparison of the binding of WW1 and WW2 domains to other putative ligands of WWOX such as p73,

PTCH1, PTPN14, SMAD7 and TMG2 (unpublished observations). In all of these cases, WW2 domain showed no intrinsic binding to any of these ligands but rather consistently enhanced ligand binding to WW1 domain between two- to three-folds. This notion is further confirmed by recent work from Aqeilan's laboratory, wherein mass spectrometry and phage display revealed that while WW1 domain bound to a plethora of new cellular partners, the WW2 domain did not apparently interact with any such ligands (34). In Table 1, a comparison of the binding of WW1 domain to various PPXY ligands of WWOX alone and in the context of WW1-WW2 tandem module is provided. It is noteworthy that such synergistic action observed here between the WW domains of WWOX appears to be a hallmark of WW tandem domains in general (35–41).

Structural insights into the physical basis underlying the ability of WW2 domain to chaperone and aid ligand binding to WW1 domain of WWOX

In order to shed light on the physical basis underlying the ability of WW2 domain to chaperone and aid ligand binding to WW1 domain, the structure of WW1-WW2 tandem module of WWOX was modeled using the NMR structure of homologous WW1-WW2 tandem module of FBP21 pre-mRNA splicing factor as a template (36). Additionally, the p73 peptide was docked into the binding groove of WW1 domain in the context of WW1-WW2 tandem module using the NMR structure of the homologous WW domain of YAP bound to a peptide containing the PPXY motif as a template (42). As shown in Figure 1, structural analysis reveals that the WW1-WW2 tandem module adopts a dumbbell-like conformation with the WW domains tethered together via what appears to be a highly flexible linker.

Notably, the p73 peptide roughly adopts the polyproline type II (PPII)-helical conformation and binds within the hydrophobic groove on the concave face of the triple-stranded β-sheet fold of WW1 domain in a canonical manner (42–45). Moreover, the p73 peptide is largely stabilized by intermolecular contacts between sidechain moieties of consensus residues P0, P+1 and Y+3 located within the PPXY motif of p73 peptide and several highly conserved residues lining the hydrophobic groove within the WW1 domain. Thus, the pyrrolidine moiety of P0, the first proline within the PPXY motif, stacks against the indole sidechain of W44 in WW1 domain. The sidechain moieties of Y33/T42 residues within the WW1 domain sandwich the pyrrolidine ring of P+1 within the PPXY motif. Finally, the phenyl moiety of Y+3, the terminal tyrosine within the PPXY motif, buries deep into the hydrophobic groove and is escorted by sidechain atoms of the A35/H37/E40 triad in WW1 domain. It is noteworthy here that the apparent lack of ligand binding to WW2 domain largely resides in the lack of conservation of W44 residue of WW1 domain in the structurally-equivalent position, occupied by Y85, within the WW2 domain (14, 32).

Of particular significance is the observation that the WW domains within the WW1-WW2 tandem module of WWOX apparently do not engage in interdomain contacts (Figure 1). Such lack of physical association between the WW domains is indeed also noted for the WW1-WW2 tandem module of FBP21 (36). Importantly, the rather flexible nature of the interdomain linker implies that the WW domains within the WW1-WW2 tandem module are unlikely to adopt a fixed spatial orientation and thus should be expected to move freely with

respect to each other. In light of such apparent lack of spatial orientation and interdomain interaction, the physical basis of how WW2 domain chaperones and augments ligand binding to WW1 domain within the WW1-WW2 tandem module of WWOX appears to be somewhat mysterious. While it is conceivable that this structural model has failed to capture the true picture of how WW domains are bundled together within the WW1-WW2 tandem module, the possibility that factors other than structure, such as protein dynamics and/or cooperativity, may hold clues to addressing this phenomenon cannot be excluded. For example, ligand binding to WW1 domain could trigger a conformational change within the WW1-WW2 tandem module so as to enhance its degrees of freedom and the resulting entropic gain could in turn lower its free energy to ligand binding.

Ligand binding to WW1 domain is coupled to the dissociation of WW2 domain within the WW1-WW2 tandem module of WWOX

To investigate the extent to which WW domains may physically associate with each other and to probe the effect of ligand binding on protein dynamics, molecular dynamics (MD) simulations were conducted on the structural model of WW1-WW2 tandem module of WWOX alone (unliganded) as well as in complex with p73 peptide (liganded) over a time scale of 2μs. It should be noted that despite their low sequence identity (~20%), the WW1-WW2 tandem module of FBP21 is ideally suited as a template to probe the extent to which the WW domains of WWOX may be physically associated in an unliganded conformation. (i) the WW domains of FBP21 are not physically associated; (ii) the WW domains of FBP21 are tethered together via a flexible linker with no defined conformation; (iii) the interdomain linkers between the WW domains of FBP21 and WWOX are of identical length (19 residues). Importantly, the starting conformation of unliganded WW1-WW2 tandem module was assumed to be identical to that of the liganded protein for the purpose of MD simulations. As shown in Figure 2, the structural superimposition of various simulated conformations suggests that the unliganded protein indeed adopts a well-defined conformation so as to allow the WW domains to physically associate with each other and attain a fixed spatial orientation relative to each other (Figure 2a). In contrast, the liganded protein seemingly samples a relatively larger conformational space so as to not only prevent a stable interaction between the WW domains but also ensure that they are able to move freely with respect to each other (Figure 2b).

To further understand the atomic basis of the physical association between WW domains within the unliganded WW1-WW2 tandem module and how ligand binding may disrupt such association, the structure of unliganded protein observed at the end of 2-μs simulation was analyzed more closely (Figure 3). Interestingly, the physical association between the WW domains in the unliganded protein is driven by the docking of the convex side of WW2 domain onto the concave face of WW1 domain. These domain-domain interactions are primarily mediated via a two-prong mechanism: firstly, the indole moiety of W44 within the WW1 domain is sandwiched by the sidechain atoms of Q65 and V73 located within WW2 domain; secondly, the sidechain group of T67 within WW2 domain is sandwiched between aromatic rings of W31 and Y33 located within WW1 domain. These van der Waals contacts are further buttressed by hydrogen bonding between the Nε1 atom of W44 within WW1

domain and Oε1 atom of Q65 within WW2 domain. Of particular note is the observation that the juxtaposition of WW2 domain on the concave face of WW1 domain partially blocks the ligand binding groove of the latter—the WW2 domain essentially acts like a “lid” that needs to be displaced in order to provide access to the incoming ligand destined to dock onto the concave face of WW1 domain. Accordingly, ligand binding must somehow result in the dissociation of WW2 domain so as to allow the WW1 domain to fully accommodate cognate ligands.

The notion that WW domains within the WW1-WW2 tandem module of WWOX physically associate with each other in the unliganded state harbors parallels with the ability of the WW2 domain of SAV1 adaptor to self-associate into a β-clam-like homodimer (46). However, the mode of dimerization of WW domains is quite distinct in each case. Thus, while the WW2 domains of SAV1 physically associate with each other in a manner akin to the palms of both hands coming together in an orthogonal manner, wherein each palm represents the concave face of the molecule harboring the ligand binding pocket. Accordingly, the WW2 homodimer of SAV1 does not bear the potential to bind ligands. In contrast, the WW domains of WWOX adopt a front-to-back mode of association, wherein the concave palm of one hand (WW1) latches onto the convex back (WW2) of the other. Interestingly, while WW2 domains of both WWOX and SAV1 share rather high sequence similarity with the WW2 domain of MAGI1, the latter predominantly adopts a monomeric conformation in solution (47), thereby implying that sequence similarity alone is a poor predictor of the ability of WW domains to dimerize. Importantly, the ability of WW domains of WWOX to physically associate and attain a fixed spatial orientation also appears to somewhat resemble the tandem WW domains of Prp40 yeast splicing factor (38). In Prp40, the interdomain linker adopts α-helical conformation, thereby imparting a relatively stable and fixed spatial orientation upon tandem WW domains. However, unlike the WW1-WW2 tandem module of WWOX, the WW domains of Prp40 do not physically associate but rather act as independent rigid bodies yet bounded together. This distinguishing feature of tandem WW domains of Prp40 is necessary in order to allow their ligand binding grooves to point outwards, thereby enabling them to bind to distinct ligands and bridge precisely between target sites within the splicing machinery.

WW1 domain of WWOX shares high sequence similarity with ubiquitin ligase family of WW domains

Sequence alignment of WW1 domain of WWOX with other WW domains within the human proteome suggests that it shares rather high sequence similarity with WW domains that belong to the E3 ubiquitin ligase family of enzymes (Figure 4). Examples include WW domains of ITCH and NEDD4 ubiquitin ligases, two of the key cellular players involved in protein turnover and degradation through the proteasome pathway (48–51). On the basis of this analysis, it is possible that the WW1 domain of WWOX may compete with cellular partners of ubiquitin ligases and, in so doing, modulate or neutralize their physiological function. Given that tumor suppressors are one of the major targets of ubiquitin ligases, the ability of WW1 domain of WWOX to compete with common cellular partners of ubiquitin ligases may have evolved as a mechanism to prevent rapid turnover and degradation of

proteins central to cellular homeostasis. Accordingly, a breakdown in this mechanism, for example due to down-expression of WWOX, may serve as a signal for normal cells to undergo oncogenic transformation. It should be noted here that the WW domains of ITCH ubiquitin ligase play a central role in the Hippo tumor suppressor pathway (22, 52, 53). It is thus also conceivable that the WW1 domain of WWOX may have a role to play in regulating the Hippo tumor suppressor pathway.

Lack of a signature tryptophan does not correlate with lack of ligand binding in WW domains

Human proteome boasts several hundred unique WW domains and they are often encountered in multiple or tandem copies in host proteins. While their occurrence as multiple copies is indicative of their cooperative action in the recognition of cognate cellular partners via multi-dentate interactions, a growing number of studies also suggest that many WW domains in the context of tandem modules act as chaperones so as to augment the structural stability and ligand binding of their neighbor (35, 37, 38). As noted above, the apparent lack of ligand binding to WW2 domain of WWOX largely resides in the lack of conservation of W44 residue of WW1 domain in the structurally-equivalent position, occupied by Y85, within the WW2 domain (14, 32). Could the ability of WW domains to have undergone evolutionary adaptation resulting in the replacement of a signature tryptophan with other amino acid residues, such as the Y85 residue in WW2 domain of WWOX (Figure 1), may have arisen out of their necessity to serve as chaperones at the expense of ligand binding? It should be noted here that this signature tryptophan, such as the W44 residue in WW1 domain of WWOX (Figure 1), forms a part of the network of residues lining the canonical hydrophobic binding groove within the triple-stranded β-sheet fold of WW domains.

In an attempt to further elaborate on the above phenomenon, the human proteome was searched in order to identify WW domains that have undergone such evolutionary change, namely the replacement of a signature tryptophan with a tyrosine within the ligand binding pocket (Figure 5). This analysis reveals that the signature tryptophan involved in ligand binding has been evolutionarily replaced by another amino acid within a substantial number of WW domains within the human proteome. Most tellingly, these WW domains can be further sub-divided depending on whether the they belong to multi-copy-WW-containing proteins (Class I) or single-copy-WW-containing proteins (Class II). But, does the simple point substitution of a signature tryptophan necessarily correlate with lack of ligand binding? While such substitution may predispose some WW domains to primarily serve as chaperones, it evidently does not appear to be universally shared among all WW domains. This notion is supported by the binding of WW4 domain of ITCH to ErbB4 (54), WW4 domain of WWP1 to ErbB4 (55), WW2 domain of MAGI1 to synaptopodin (56), and WW2 domain of SMURF1/2 to MDM2 (57), all of which harbor either a tyrosine or phenylalanine in place of the signature tryptophan. The foregoing argument suggests that WW domains that harbor a pair of signature tryptophan residues should not be taken for granted as they could also lack physiological ligands. In short, further work on structural characterization of WW domains should lead to formulation of rules that underpin their ability to act as orphan

domains whose sole role in cellular signaling is to chaperone and aid ligand binding to tandem partners.

SDR domain of WWOX appears to serve as a retinal oxidoreductase

Although the ability of WWOX to interact with a wide variety of cellular proteins via its WW1 domain is well-established (13–17, 33), the molecular function of its SDR domain remains hitherto unexplored. It is noteworthy that the SDR family of enzymes constitutes one of the largest protein superfamilies identified to date. The human genome encodes ~100 members of the SDR family that catalyze NAD(P)(H)-dependent oxido-redox reactions for a wide variety of cellular substrates such as steroids and retinoids (58). One of the best characterized members of the human SDR family is the 17β-hydroxysteroid dehydrogenase 1 (HSD1) (59), which catalyzes the reversible reduction of estrone to estradiol using NADPH as a reducing agent (60–63):

$$\mathrm{Estrone}+\mathrm{NADPH}<=>\mathrm{Estradiol}+\mathrm{NADP}^{+}$$

Given that estradiol serves as a ligand for the activation of ERα coupled with the fact that HSD1 is overexpressed in breast cancer (61, 64), HSD1 remains an important target for anti-estrogen therapy. Importantly, due to the strong correlation between cellular expression of ERα and WWOX in breast cancer (5, 9, 65), it has been suggested that the SDR domain of WWOX may be involved in the synthesis of estradiol from estrone or vice versa in a manner akin to the action of HSD1. Interestingly, recent studies by Bednarek and co-workers have suggested that the SDR domain of WWOX may indeed be involved in steroid metabolism (66). However, this analysis was conducted in whole cell lysates in lieu of an isolated recombinant protein, prompting reductionists and biophysicists-alike to question the validity of these data. Of particular concern is the fact that the SDR domain of WWOX shares rather poor amino acid sequence similarity with other members of steroid dehydrogenases such as HSD1/2/3 involved in steroid metabolism.

In an effort to resolve the ongoing controversy vis-à-vis the precise enzymatic function of WWOX, an extensive in silico analysis was conducted to compare the amino acid sequence alignment of the SDR domain of WWOX with other members of the SDR family. This analysis indicates that of all the ~100 members of the SDR family, the SDR domain of WWOX harbors the most optimal sequence alignment with not only members of the human retinol dehydrogenases such as RDH11, RDH12 and RDH13 but also with those of prokaryotes such as mpRDH from Mycobacterium paratuberculosis (Figure 6). As their name implies, the members of the retinol dehydrogenase family are typically involved in oxidoreductive catalysis of retinoids such as retinol, retinal and retinoic acid using NADP(H)($^{+}$) as a reducing/oxidizing agent (67–70):

$$\mathrm{Retinol}+\mathrm{NADP}^{+}<=>\mathrm{Retinal}+\mathrm{NADPH}$$

Most remarkably, the rather high sequence similarity between the SDR domain of WWOX and retinol dehydrogenases is further buoyed by the presence of various highly conserved

catalytic motifs in virtually identical positions. These include the GXXXGXG motif that is involved in accommodating the $NADP^+$/NADPH cofactor, while the YXXXK consensus sequence represents the active site motif critical for the enzymatic activity of SDR domains. Additionally, an absolutely conserved serine (S260 in WWOX) is required for the stabilization of retinoid substrate within the active site. While still in preliminary stage, biochemical studies conducted on a high-quality bacterially-purified recombinant protein in my laboratory indeed confirm that the SDR domain of WWOX is a bona fide retinal oxidoreductase—not only does it catalyze the oxidation of retinol to retinal aldehyde but it also appears to efficiently catalyze the reversible reaction. Equally importantly, these preliminary in vitro studies suggest that the SDR domain of WWOX may also be involved in the oxidative catalysis of retinal to retinoic acid.

SDR domain of WWOX adopts a canonical dehydrogenase catalytic fold

To provide further evidence in support of the hypothesis that WWOX likely serves as a retinal oxidoreductase in cellular signaling, the structure of its catalytic SDR domain was modeled in complex with the NADPH co-factor and all-trans-retinal substrate (Figure 7). Such analysis shows that the SDR domain adopts a canonical Rossmann fold that is shared by a wide variety of nucleotide-binding proteins such as the dehydrogenases. In particular, the SDR domain of WWOX is comprised of a central seven-stranded parallel β-sheet sandwiched between three α-helices on one face and four α-helices on the other side. The YXXXK active site motif, where Y and K are respectively Y293 and K297, as well as the co-factor (NADPH) and the substrate (retinal) binding sites are clustered together in a deep cleft on one opening of the β-sandwich. This molecular design of the catalytic center should thus not only provide specificity but also afford a smooth entry and exit for both the co-factor and the substrate during each step of catalysis.

Importantly, the Y293 and K297 active site residues act as general acid and base in mediating the reductive and oxidative catalysis, respectively. As schematically proposed in Figure 8, on the basis of catalytic action of other well-characterized dehydrogenases (71, 72), the reduction reaction begins with the nucleophilic attack on the carbonyl carbon (C15) atom of retinal by one of the hydrogen atoms attached to the ring carbon (C4N) atom of nicotinamide moiety of NADPH leading to the generation of oxidized $NADP^+$. This is followed by the stripping of a proton from the hydroxyl oxygen (Oη) atom of Y293 by the carbonyl oxygen (O1) atom of retinal, thereby generating retinol. The release of a proton by the hydroxyl oxygen (Oη) atom of Y293 is facilitated by the donation of a proton by the protonated amino nitrogen (Nζ) atom of K297. Finally, the net positive charge on the amino nitrogen atom (Nζ) atom of K297 is restored by the donation of a proton from water solvent and the concomitant generation of a hydroxyl ion. On the other hand, the oxidation reaction begins with the nucleophilic attack on the ring carbon (C4N) atom of nicotinamide moiety of $NADP^+$ by one of the hydrogen atoms attached to the hydroxyl carbon (C15) atom of retinol, thereby resulting in the release of reduced NADPH. This is facilitated by the donation of a lone pair of electrons from the hydroxyl oxygen (Oη) atom of Y293 to the hydroxyl hydrogen atom of retinol followed by the formation of carbonyl double bond, thereby leading to the production of retinal. The ability of Y293 to serve as a proton acceptor is aided by the stripping of its hydroxyl proton by the amino nitrogen (Nζ) atom of

K297, which in turn releases a proton to the free hydroxyl ion to produce one molecule of water solvent.

Future Perspectives

While a vast majority of efforts have been directed at studying the cellular and tumor biology of WWOX over the past decade or so, recent work from my laboratory is beginning to shed new light on structure-function relationships in this important and rapidly emerging cellular player. In this review, the latest insights into the structural plasticity observed between the WW domains of WWOX in their ability to positively cooperate so as to enable WWOX to mediate an array of cellular signaling cascades have been highlighted (13–17, 33). Additionally, an in-depth in silico analysis, that is further supported by our preliminary in vitro studies, has been provided in order to provoke the notion that the SDR domain of WWOX is a retinal oxidoreductase and thus it is likely to be involved in retinoid metabolism. It is noteworthy that retinoids play a central role in cellular homeostasis and are being increasingly used as therapeutic agents to combat cancer, particularly leukemia (73). More importantly, it is conceivable that WWOX plays a key role in the development and etiology of human vision in light of the role of retinal as a ligand for the rhodopsin photoreceptor. Indeed, WWOX is not only richly expressed in the inner retina at perinatal stage but it is also overexpressed in the retinal ganglion cells in adults (74–76). Additionally, mitochondrial and nuclear translocation of WWOX has been linked to light-induced retinal damage (76).

Given that retinal serves as a precursor for retinoic acid, an active derivative of Vitamin A, it is also plausible that WWOX plays a role in regulating the action of retinoic acid receptors (RARs) (77, 78). RARs are ligand-gated transcription factors that belong to the nuclear receptor family (79–83). Upon their activation with retinoic acid, RARs translocate to the nucleus and bind to promoters of target genes, thereby directly regulating gene expression. In this manner, RARs modulate a wide variety of cellular processes, including embryonic development, cell growth arrest, differentiation and apoptosis. Accordingly, the ability of WWOX to modulate the cellular level of retinoic acid would directly serve as a key regulatory switch for the action of downstream RARs, whose transcriptional activity is directly dependent upon the supply of retinoic acid. For example, WWOX-mediated oxidation of retinal to retinoic acid would be expected to stimulate the transcriptional activity of RARs. On the other hand, WWOX-driven reduction of retinal to retinol would seemingly lower cellular levels of retinoic acid, thereby down-regulating the action of RARs. The decision to whether WWOX stimulates or suppresses transcriptional activity of RARs would in turn depend upon the redox state of the cell, primarily the supply of oxidizing ($NAD[P]^+$) versus reducing (NAD[P]H) cofactors. In this context, WWOX would link the action of RARs to other ongoing events within the cell and thereby provide a tight homeostatometer of cellular environment. Given that RARs play a central role in the homeostatic equilibrium between mitogenic and anti-proliferative cellular activities (84), the ability of WWOX to directly affect their transcriptional activity would appear to be a novel signaling pathway by which WWOX exerts its tumor suppressor function in many cancers, including those of breast and prostate (5–12).

In sum, the evidence and arguments presented in this review strongly warrant further experimental investigations into the link between WWOX and cellular cascades involved in human vision as well as in retinoic acid signaling. In particular, the extent to which exposure of cultured mammalian cells to retinal affects cellular expression levels of WWOX would provide further clues into the link between WWOX and retinoid metabolism. On the other hand, siRNA-mediated knockdown of WWOX should shed new light on the extent to which WWOX mediates the transcriptional activity of RARs. Finally, in vivo studies on the effect of retinal on WWOX-deficient versus normal mice would also be important to establish a direct link between WWOX and retinoid metabolism.

Acknowledgments

This work was supported by the National Institutes of Health Grant R01-GM083897 and funds from the Sylvester Comprehensive Cancer Center.

I am grateful to Brett Schuchardt for collecting some of the preliminary data discussed here and for many thoughtful discussions.

ABBREVIATIONS

ErbB4	Erythroblastic (Erb) leukemia viral oncogene homolog B4
ERα	Estrogen receptor alpha
FBP21	Formin-binding protein 21
mpRDH	Retinol dehydrogenase (from Mycobacterium paratuberculosis)
NADP	Nicotinamide adenine dinucleotide phosphate (oxidized)
NADPH	Nicotinamide adenine dinucleotide phosphate (reduced)
p73	Tumor protein 73
PPII	Polyproline type II (helix)
PTCH1	Protein patched homolog 1
PTPN14	Protein tyrosine phosphatase (non-receptor type) 14
SDR	Short-chain dehydrogenase/reductase
SMAD7	Mothers against decapentaplegic homolog 7
TMG2	Transmembrane gamma-carboxyglutamic acid protein 2
YAP	YES-associated protein
WBP1/2	WW domain-binding proteins 1 and 2
WWOX	WW domain-containing oxidoreductase

References

1. Bednarek AK, Laflin KJ, Daniel RL, Liao Q, Hawkins KA, Aldaz CM. WWOX, a novel WW domain-containing protein mapping to human chromosome 16q23.3-24.1, a region frequently affected in breast cancer. Cancer Res. 2000; 60:2140–2145. [PubMed: 10786676]

2. Bednarek AK, Keck-Waggoner CL, Daniel RL, Laflin KJ, Bergsagel PL, Kiguchi K, Brenner AJ, Aldaz CM. WWOX, the FRA16D gene, behaves as a suppressor of tumor growth. Cancer Res. 2001; 61:8068–8073. [PubMed: 11719429]

3. Hezova R, Ehrmann J, Kolar Z. WWOX, a new potential tumor suppressor gene. Biomed Pap Med Fac Univ Palacky Olomouc Czech Repub. 2007; 151:11–15. [PubMed: 17690733]

4. Gardenswartz A, Aqeilan RI. WW domain-containing oxidoreductase's role in myriad cancers: clinical significance and future implications. Exp Biol Med (Maywood). 2014; 239:253–263. [PubMed: 24510053]

5. Nunez MI, Ludes-Meyers J, Abba MC, Kil H, Abbey NW, Page RE, Sahin A, Klein-Szanto AJ, Aldaz CM. Frequent loss of WWOX expression in breast cancer: correlation with estrogen receptor status. Breast Cancer Res Treat. 2005; 89:99–105. [PubMed: 15692750]

6. Aqeilan RI, Kuroki T, Pekarsky Y, Albagha O, Trapasso F, Baffa R, Huebner K, Edmonds P, Croce CM. Loss of WWOX expression in gastric carcinoma. Clin Cancer Res. 2004; 10:3053–3058. [PubMed: 15131042]

7. Aqeilan RI, Croce CM. WWOX in biological control and tumorigenesis. J Cell Physiol. 2007; 212:307–310. [PubMed: 17458891]

8. Aqeilan RI, Hagan JP, Aqeilan HA, Pichiorri F, Fong LY, Croce CM. Inactivation of the Wwox gene accelerates forestomach tumor progression in vivo. Cancer Res. 2007; 67:5606–5610. [PubMed: 17575124]

9. Pluciennik E, Kusinska R, Potemski P, Kubiak R, Kordek R, Bednarek AK. WWOX--the FRA16D cancer gene: expression correlation with breast cancer progression and prognosis. Eur J Surg Oncol. 2006; 32:153–157. [PubMed: 16360296]

10. Lewandowska U, Zelazowski M, Seta K, Byczewska M, Pluciennik E, Bednarek AK. WWOX, the tumour suppressor gene affected in multiple cancers. J Physiol Pharmacol. 2009; 60(Suppl 1):47–56. [PubMed: 19609013]

11. Zelazowski MJ, Pluciennik E, Pasz-Walczak G, Potemski P, Kordek R, Bednarek AK. WWOX expression in colorectal cancer--a real-time quantitative RT-PCR study. Tumour Biol. 2011; 32:551–560. [PubMed: 21347750]

12. Sudol M, Hunter T. NeW wrinkles for an old domain. Cell. 2000; 103:1001–1004. [PubMed: 11163176]

13. Ludes-Meyers JH, Kil H, Bednarek AK, Drake J, Bedford MT, Aldaz CM. WWOX binds the specific proline-rich ligand PPXY: identification of candidate interacting proteins. Oncogene. 2004; 23:5049–5055. [PubMed: 15064722]

14. McDonald CB, Buffa L, Bar-Mag T, Salah Z, Bhat V, Mikles DC, Deegan BJ, Seldeen KL, Malhotra A, Sudol M, Aqeilan RI, Nawaz Z, Farooq A. Biophysical basis of the binding of WWOX tumor suppressor to WBP1 and WBP2 adaptors. J Mol Biol. 2012; 422:58–74. [PubMed: 22634283]

15. Aqeilan RI, Donati V, Palamarchuk A, Trapasso F, Kaou M, Pekarsky Y, Sudol M, Croce CM. WW domain-containing proteins, WWOX and YAP, compete for interaction with ErbB-4 and modulate its transcriptional function. Cancer Res. 2005; 65:6764–6772. [PubMed: 16061658]

16. Aqeilan RI, Pekarsky Y, Herrero JJ, Palamarchuk A, Letofsky J, Druck T, Trapasso F, Han SY, Melino G, Huebner K, Croce CM. Functional association between Wwox tumor suppressor protein and p73, a p53 homolog. Proc Natl Acad Sci U S A. 2004; 101:4401–4406. [PubMed: 15070730]

17. Del Mare S, Salah Z, Aqeilan RI. WWOX: its genomics, partners, and functions. J Cell Biochem. 2009; 108:737–745. [PubMed: 19708029]

18. Zhao B, Wei X, Li W, Udan RS, Yang Q, Kim J, Xie J, Ikenoue T, Yu J, Li L, Zheng P, Ye K, Chinnaiyan A, Halder G, Lai ZC, Guan KL. Inactivation of YAP oncoprotein by the Hippo pathway is involved in cell contact inhibition and tissue growth control. Genes Dev. 2007; 21:2747–2761. [PubMed: 17974916]

19. Bertini E, Oka T, Sudol M, Strano S, Blandino G. YAP: at the crossroad between transformation and tumor suppression. Cell Cycle. 2009; 8:49–57. [PubMed: 19106601]

20. Sudol M. Newcomers to the WW Domain-Mediated Network of the Hippo Tumor Suppressor Pathway. Genes Cancer. 2010; 1:1115–1118. [PubMed: 21779434]

21. Sudol M, Harvey KF. Modularity in the Hippo signaling pathway. Trends Biochem Sci. 2010; 35:627–633. [PubMed: 20598891]
22. Salah Z, Aqeilan RI. WW domain interactions regulate the Hippo tumor suppressor pathway. Cell Death Dis. 2011; 2:e172. [PubMed: 21677687]
23. Chen HI, Sudol M. The WW domain of Yes-associated protein binds a proline-rich ligand that differs from the consensus established for Src homology 3-binding modules. Proc Natl Acad Sci U S A. 1995; 92:7819–7823. [PubMed: 7644498]
24. Chen HI, Einbond A, Kwak SJ, Linn H, Koepf E, Peterson S, Kelly JW, Sudol M. Characterization of the WW domain of human yes-associated protein and its polyproline-containing ligands. J Biol Chem. 1997; 272:17070–17077. [PubMed: 9202023]
25. Komuro A, Nagai M, Navin NE, Sudol M. WW domain-containing protein YAP associates with ErbB-4 and acts as a co-transcriptional activator for the carboxyl-terminal fragment of ErbB-4 that translocates to the nucleus. J Biol Chem. 2003; 278:33334–33341. [PubMed: 12807903]
26. Omerovic J, Puggioni EM, Napoletano S, Visco V, Fraioli R, Frati L, Gulino A, Alimandi M. Ligand-regulated association of ErbB-4 to the transcriptional co-activator YAP65 controls transcription at the nuclear level. Exp Cell Res. 2004; 294:469–479. [PubMed: 15023535]
27. Levy D, Adamovich Y, Reuven N, Shaul Y. Yap1 phosphorylation by c-Abl is a critical step in selective activation of proapoptotic genes in response to DNA damage. Mol Cell. 2008; 29:350–361. [PubMed: 18280240]
28. Kulman JD, Harris JE, Xie L, Davie EW. Proline-rich Gla protein 2 is a cell-surface vitamin K-dependent protein that binds to the transcriptional coactivator Yes-associated protein. Proc Natl Acad Sci U S A. 2007; 104:8767–8772. [PubMed: 17502622]
29. Liu X, Yang N, Figel SA, Wilson KE, Morrison CD, Gelman IH, Zhang J. PTPN14 interacts with and negatively regulates the oncogenic function of YAP. Oncogene. 2013; 32:1266–1273. [PubMed: 22525271]
30. Ferrigno O, Lallemand F, Verrecchia F, L'Hoste S, Camonis J, Atfi A, Mauviel A. Yes-associated protein (YAP65) interacts with Smad7 and potentiates its inhibitory activity against TGF-beta/Smad signaling. Oncogene. 2002; 21:4879–4884. [PubMed: 12118366]
31. Linn H, Ermekova KS, Rentschler S, Sparks AB, Kay BK, Sudol M. Using molecular repertoires to identify high-affinity peptide ligands of the WW domain of human and mouse YAP. Biol Chem. 1997; 378:531–537. [PubMed: 9224934]
32. Schuchardt BJ, Bhat V, Mikles DC, McDonald CB, Sudol M, Farooq A. Molecular origin of the binding of WWOX tumor suppressor to ErbB4 receptor tyrosine kinase. Biochemistry. 2013; 52:9223–9236. [PubMed: 24308844]
33. Aqeilan RI, Palamarchuk A, Weigel RJ, Herrero JJ, Pekarsky Y, Croce CM. Physical and functional interactions between the Wwox tumor suppressor protein and the AP-2gamma transcription factor. Cancer Res. 2004; 64:8256–8261. [PubMed: 15548692]
34. Abu-Odeh M, Bar-Mag T, Huang H, Kim T, Salah Z, Abdeen SK, Sudol M, Reichmann D, Sidhu S, Kim PM, Aqeilan RI. Characterizing WW domain interactions of tumor suppressor WWOX reveals its association with multiprotein networks. J Biol Chem. 2014; 289:8865–8880. [PubMed: 24550385]
35. Sudol M, Recinos CC, Abraczinskas J, Humbert J, Farooq A. WW or WoW: the WW domains in a union of bliss. IUBMB Life. 2005; 57:773–778. [PubMed: 16393779]
36. Huang X, Beullens M, Zhang J, Zhou Y, Nicolaescu E, Lesage B, Hu Q, Wu J, Bollen M, Shi Y. Structure and function of the two tandem WW domains of the pre-mRNA splicing factor FBP21 (formin-binding protein 21). J Biol Chem. 2009; 284:25375–25387. [PubMed: 19592703]
37. Fedoroff OY, Townson SA, Golovanov AP, Baron M, Avis JM. The Structure and Dynamics of Tandem WW Domains in a Negative Regulator of Notch Signaling, Suppressor of Deltex. J Biol Chem. 2004; 279:34991–35000. [PubMed: 15173166]
38. Wiesner S, Stier G, Sattler M, Macias MJ. Solution Structure and Ligad Recognition of the WW Domain of the Yeast Splicing Factor Prp40. J Mol Biol. 2002; 324:807–822. [PubMed: 12460579]
39. Kanelis V, Farrow NA, Kay LE, Rotin D, Forman-Kay JD. NMR studies of tandem WW domains of Nedd4 in complex with a PY motif-containing region of the epithelial sodium channel. Biochem Cell Biol. 1998; 76:341–350. [PubMed: 9923703]

40. Chong PA, Lin H, Wrana JL, Forman-Kay JD. Coupling of tandem Smad ubiquitination regulatory factor (Smurf) WW domains modulates target specificity. Proc Natl Acad Sci U S A. 2010; 107:18404–18409. [PubMed: 20937913]
41. Webb C, Upadhyay A, Giuntini F, Eggleston I, Furutani-Seiki M, Ishima R, Bagby S. Structural features and ligand binding properties of tandem WW domains from YAP and TAZ, nuclear effectors of the Hippo pathway. Biochemistry. 2011; 50:3300–3309. [PubMed: 21417403]
42. Pires JR, Taha-Nejad F, Toepert F, Ast T, Hoffmuller U, Schneider-Mergener J, Kuhne R, Macias MJ, Oschkinat H. Solution structures of the YAP65 WW domain and the variant L30 K in complex with the peptides GTPPPPYTVG, N-(n-octyl)-GPPPY and PLPPY and the application of peptide libraries reveal a minimal binding epitope. J Mol Biol. 2001; 314:1147–1156. [PubMed: 11743730]
43. Macias MJ, Hyvonen M, Baraldi E, Schultz J, Sudol M, Saraste M, Oschkinat H. Structure of the WW domain of a kinase-associated protein complexed with a proline-rich peptide. Nature. 1996; 382:646–649. [PubMed: 8757138]
44. Huang X, Poy F, Zhang R, Joachimiak A, Sudol M, Eck MJ. Structure of a WW domain containing fragment of dystrophin in complex with beta-dystroglycan. Nat Struct Biol. 2000; 7:634–638. [PubMed: 10932245]
45. Kanelis V, Rotin D, Forman-Kay JD. Solution structure of a Nedd4 WW domain-ENaC peptide complex. Nat Struct Biol. 2001; 8:407–412. [PubMed: 11323714]
46. Ohnishi S, Guntert P, Koshiba S, Tomizawa T, Akasaka R, Tochio N, Sato M, Inoue M, Harada T, Watanabe S, Tanaka A, Shirouzu M, Kigawa T, Yokoyama S. Solution structure of an atypical WW domain in a novel beta-clam-like dimeric form. FEBS Lett. 2007; 581:462–468. [PubMed: 17239860]
47. Ohnishi S, Tochio N, Tomizawa T, Akasaka R, Harada T, Seki E, Sato M, Watanabe S, Fujikura Y, Koshiba S, Terada T, Shirouzu M, Tanaka A, Kigawa T, Yokoyama S. Structural basis for controlling the dimerization and stability of the WW domains of an atypical subfamily. Protein Sci. 2008; 17:1531–1541. [PubMed: 18562638]
48. Chastagner P, Israel A, Brou C. AIP4/Itch regulates Notch receptor degradation in the absence of ligand. PLoS One. 2008; 3:e2735. [PubMed: 18628966]
49. Chastagner P, Israel A, Brou C. Itch/AIP4 mediates Deltex degradation through the formation of K29-linked polyubiquitin chains. EMBO Rep. 2006; 7:1147–1153. [PubMed: 17028573]
50. Lin Q, Wang J, Childress C, Sudol M, Carey DJ, Yang W. HECT E3 ubiquitin ligase Nedd4-1 ubiquitinates ACK and regulates epidermal growth factor (EGF)-induced degradation of EGF receptor and ACK. Mol Cell Biol. 2010; 30:1541–1554. [PubMed: 20086093]
51. Pham N, Rotin D. Nedd4 regulates ubiquitination and stability of the guanine-nucleotide exchange factor CNrasGEF. J Biol Chem. 2001; 276:46995–47003. [PubMed: 11598133]
52. Salah Z, Melino G, Aqeilan RI. Negative regulation of the Hippo pathway by E3 ubiquitin ligase ITCH is sufficient to promote tumorigenicity. Cancer Res. 2011; 71:2010–2020. [PubMed: 21212414]
53. Ho KC, Zhou Z, She YM, Chun A, Cyr TD, Yang X. Itch E3 ubiquitin ligase regulates large tumor suppressor 1 stability. Proc Natl Acad Sci U S A. 2011; 108:4870–4875. [PubMed: 21383157]
54. Omerovic J, Santangelo L, Puggioni EM, Marrocco J, Dall'Armi C, Palumbo C, Belleudi F, Di Marcotullio L, Frati L, Torrisi MR, Cesareni G, Gulino A, Alimandi M. The E3 ligase Aip4/Itch ubiquitinates and targets ErbB-4 for degradation. FASEB J. 2007; 21:2849–2862. [PubMed: 17463226]
55. Li Y, Zhou Z, Alimandi M, Chen C. WW domain containing E3 ubiquitin protein ligase 1 targets the full-length ErbB4 for ubiquitin-mediated degradation in breast cancer. Oncogene. 2009; 28:2948–2958. [PubMed: 19561640]
56. Patrie KM, Drescher AJ, Welihinda A, Mundel P, Margolis B. Interaction of two actin-binding proteins, synaptopodin and alpha-actinin-4, with the tight junction protein MAGI-1. J Biol Chem. 2002; 277:30183–30190. [PubMed: 12042308]
57. Nie J, Xie P, Liu L, Xing G, Chang Z, Yin Y, Tian C, He F, Zhang L. Smad ubiquitylation regulatory factor 1/2 (Smurf1/2) promotes p53 degradation by stabilizing the E3 ligase MDM2. J Biol Chem. 2010; 285:22818–22830. [PubMed: 20484049]

58. Bray JE, Marsden BD, Oppermann U. The human short-chain dehydrogenase/reductase (SDR) superfamily: a bioinformatics summary. Chem Biol Interact. 2009; 178:99–109. [PubMed: 19061874]

59. Breton R, Housset D, Mazza C, Fontecilla-Camps JC. The structure of a complex of human 17beta-hydroxysteroid dehydrogenase with estradiol and NADP+ identifies two principal targets for the design of inhibitors. Structure. 1996; 4:905–915. [PubMed: 8805577]

60. Nguyen BL, Chetrite G, Pasqualini JR. Transformation of estrone and estradiol in hormone-dependent and hormone-independent human breast cancer cells. Effects of the antiestrogen ICI 164,384, danazol, and promegestone (R-5020). Breast Cancer Res Treat. 1995; 34:139–146. [PubMed: 7647331]

61. Pasqualini JR. The selective estrogen enzyme modulators in breast cancer: a review. Biochim Biophys Acta. 2004; 1654:123–143. [PubMed: 15172700]

62. Aka JA, Mazumdar M, Lin SX. Reductive 17beta-hydroxysteroid dehydrogenases in the sulfatase pathway: critical in the cell proliferation of breast cancer. Mol Cell Endocrinol. 2009; 301:183–190. [PubMed: 19038308]

63. Poutanen M, Isomaa V, Peltoketo H, Vihko R. Role of 17 beta-hydroxysteroid dehydrogenase type 1 in endocrine and intracrine estradiol biosynthesis. J Steroid Biochem Mol Biol. 1995; 55:525–532. [PubMed: 8547177]

64. Vermeulen A, Deslypere JP, Paridaens R. Steroid dynamics in the normal and carcinomatous mammary gland. J Steroid Biochem. 1986; 25:799–802. [PubMed: 3027457]

65. Nunez MI, Rosen DG, Ludes-Meyers JH, Abba MC, Kil H, Page R, Klein-Szanto AJ, Godwin AK, Liu J, Mills GB, Aldaz CM. WWOX protein expression varies among ovarian carcinoma histotypes and correlates with less favorable outcome. BMC Cancer. 2005; 5:64. [PubMed: 15982416]

66. Saluda-Gorgul A, Seta K, Nowakowska M, Bednarek AK. WWOX oxidoreductase--substrate and enzymatic characterization. Z Naturforsch C. 2011; 66:73–82. [PubMed: 21476439]

67. Gough WH, VanOoteghem S, Sint T, Kedishvili NY. cDNA cloning and characterization of a new human microsomal NAD+-dependent dehydrogenase that oxidizes all-trans-retinol and 3alpha-hydroxysteroids. J Biol Chem. 1998; 273:19778–19785. [PubMed: 9677409]

68. Kedishvili NY, Chumakova OV, Chetyrkin SV, Belyaeva OV, Lapshina EA, Lin DW, Matsumura M, Nelson PS. Evidence that the human gene for prostate short-chain dehydrogenase/reductase (PSDR1) encodes a novel retinal reductase (RalR1). J Biol Chem. 2002; 277:28909–28915. [PubMed: 12036956]

69. Thompson DA, Janecke AR, Lange J, Feathers KL, Hubner CA, McHenry CL, Stockton DW, Rammesmayer G, Lupski JR, Antinolo G, Ayuso C, Baiget M, Gouras P, Heckenlively JR, den Hollander A, Jacobson SG, Lewis RA, Sieving PA, Wissinger B, Yzer S, Zrenner E, Utermann G, Gal A. Retinal degeneration associated with RDH12 mutations results from decreased 11-cis retinal synthesis due to disruption of the visual cycle. Hum Mol Genet. 2005; 14:3865–3875. [PubMed: 16269441]

70. Haeseleer F, Jang GF, Imanishi Y, Driessen CA, Matsumura M, Nelson PS, Palczewski K. Dual-substrate specificity short chain retinol dehydrogenases from the vertebrate retina. J Biol Chem. 2002; 277:45537–45546. [PubMed: 12226107]

71. Yao Y, Han W-W, Zhou Y-H, Luo Q, Li Z-S. Catalytic Mechanism of Human Photoreceptor Retinol Dehydrogenase: A Theoretic Study. J Theor Comput Chem. 2008; 7:565–571.

72. Hou R, Chen Z, Yi X, Blan J, Xu G. Catalytic reaction mechanism of L-lactate dehydrogenase: an ab initio study. Sci China (Series B). 2000; 43:587–599.

73. Elbahesh E, Patel N, Tabbara IA. Treatment of acute promyelocytic leukemia. Anticancer Res. 2014; 34:1507–1517. [PubMed: 24692677]

74. Bonfanti L, Candeo P, Piccinini M, Carmignoto G, Comelli MC, Ghidella S, Bruno R, Gobetto A, Merighi A. Distribution of protein gene product 9.5 (PGP 9.5) in the vertebrate retina: evidence that immunoreactivity is restricted to mammalian horizontal and ganglion cells. J Comp Neurol. 1992; 322:35–44. [PubMed: 1430309]

75. Xiang M, Zhou L, Macke JP, Yoshioka T, Hendry SH, Eddy RL, Shows TB, Nathans J. The Brn-3 family of POU-domain factors: primary structure, binding specificity, and expression in subsets of

retinal ganglion cells and somatosensory neurons. J Neurosci. 1995; 15:4762–4785. [PubMed: 7623109]

76. Chen ST, Chuang JI, Cheng CL, Hsu LJ, Chang NS. Light-induced retinal damage involves tyrosine 33 phosphorylation, mitochondrial and nuclear translocation of WW domain-containing oxidoreductase in vivo. Neuroscience. 2005; 130:397–407. [PubMed: 15664696]
77. Germain P, Chambon P, Eichele G, Evans RM, Lazar MA, Leid M, De Lera AR, Lotan R, Mangelsdorf DJ, Gronemeyer H. International Union of Pharmacology. LX. Retinoic acid receptors. Pharmacol Rev. 2006; 58:712–725. [PubMed: 17132850]
78. Allenby G, Bocquel MT, Saunders M, Kazmer S, Speck J, Rosenberger M, Lovey A, Kastner P, Grippo JF, Chambon P, et al. Retinoic acid receptors and retinoid X receptors: interactions with endogenous retinoic acids. Proc Natl Acad Sci U S A. 1993; 90:30–34. [PubMed: 8380496]
79. Evans RM. The steroid and thyroid hormone receptor superfamily. Science. 1988; 240:889–895. [PubMed: 3283939]
80. Escriva H, Bertrand S, Laudet V. The evolution of the nuclear receptor superfamily. Essays Biochem. 2004; 40:11–26. [PubMed: 15242336]
81. Thornton JW. Evolution of vertebrate steroid receptors from an ancestral estrogen receptor by ligand exploitation and serial genome expansions. Proc Natl Acad Sci U S A. 2001; 98:5671–5676. [PubMed: 11331759]
82. McKenna NJ, Cooney AJ, DeMayo FJ, Downes M, Glass CK, Lanz RB, Lazar MA, Mangelsdorf DJ, Moore DD, Qin J, Steffen DL, Tsai MJ, Tsai SY, Yu R, Margolis RN, Evans RM, O'Malley BW. Minireview: Evolution of NURSA, the Nuclear Receptor Signaling Atlas. Mol Endocrinol. 2009; 23:740–746. [PubMed: 19423650]
83. Evans RM, Mangelsdorf DJ. Nuclear Receptors, RXR, and the Big Bang. Cell. 2014; 157:255–266. [PubMed: 24679540]
84. Duong V, Rochette-Egly C. The molecular physiology of nuclear retinoic acid receptors. From health to disease. Biochim Biophys Acta. 2011; 1812:1023–1031. [PubMed: 20970498]
85. Marti-Renom MA, Stuart AC, Fiser A, Sanchez R, Melo F, Sali A. Comparative Protein Structure Modeling of Genes and Genomes. Annu Rev Biophys Biomol Struct. 2000; 29:291–325. [PubMed: 10940251]
86. Carson M. Ribbons 2.0. J Appl Crystallogr. 1991; 24:958–961.
87. Van Der Spoel D, Lindahl E, Hess B, Groenhof G, Mark AE, Berendsen HJ. GROMACS: fast, flexible, and free. J Comput Chem. 2005; 26:1701–1718. [PubMed: 16211538]
88. Lindorff-Larsen K, Piana S, Palmo K, Maragakis P, Klepeis JL, Dror RO, Shaw DE. Improved side-chain torsion potentials for the Amber ff99SB protein force field. Proteins. 2010; 78:1950–1958. [PubMed: 20408171]
89. Hornak V, Abel R, Okur A, Strockbine B, Roitberg A, Simmerling C. Comparison of multiple Amber force fields and development of improved protein backbone parameters. Proteins. 2006; 65:712–725. [PubMed: 16981200]
90. Koradi R, Billeter M, Wuthrich K. MOLMOL: a program for display and analysis of macromolecular structures. J Mol Graph. 1996; 14:51–55. [PubMed: 8744573]

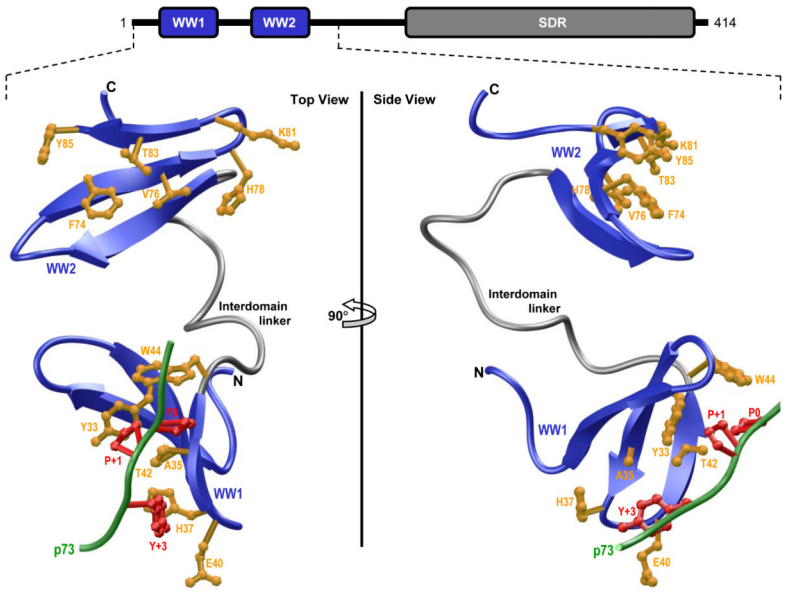

Figure 1.

Ribbon representation of the structural model of WW1-WW2 tandem module of WWOX in complex with the p73 peptide containing the PPXY motif bound to the WW1 domain. Two alternative orientations related by a 90°-rotation about the vertical axis are depicted for the inquisitive eye. In each case, the WW domains are shown in blue with the interdomain linker depicted in gray, and the bound peptide is colored green. The sidechain moieties of residues (yellow) within the WW1 domain engaged in intermolecular contacts with the consensus residues (red) within the PPXY motif of p73 peptide are shown. For comparison, the sidechain moieties of structurally-equivalent residues (yellow) within the putative ligand binding groove of WW2 domain are also depicted. Note that the modular architecture of WWOX is overlaid to indicate the relative locations of the N-terminal WW1-WW2 tandem module and the C-terminal SDR domain. The structural model of the WW1-WW2 tandem module was built using the MODELLER software based on homology modeling (85). The unliganded model was obtained using the NMR structure of WW1-WW2 tandem module of FBP21 pre-mRNA splicing factor as a template (PDBID 2JXW). To obtain the liganded model, the 12-mer p73 peptide (HCTPPPPYHADP) was docked onto the WW1 domain within the unliganded structure of WW1-WW2 tandem module in a 1:1 stoichiometry using the NMR structure of the homologous WW domain of YAP bound to a peptide containing the PPXY motif as a template (PDBID 1JMQ). The structural model was rendered using RIBBONS (86).

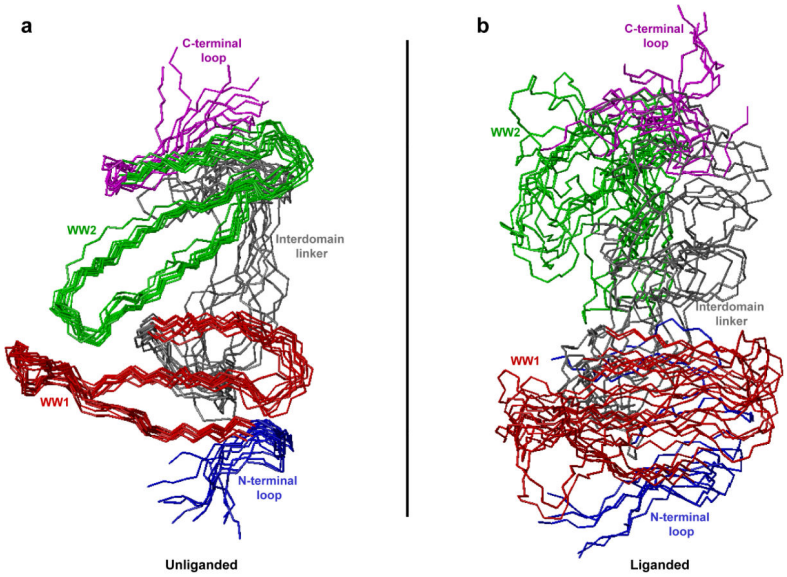

Figure 2.

Superimposition of simulated structures as derived from molecular dynamics (MD) analysis conducted on the structural model of WW1-WW2 tandem module of WWOX alone (unliganded) and in complex with p73 peptide containing the PPXY motif bound to the WW1 domain (liganded). Note that the superimposed structures for the unliganded (a) and liganded (b) WW1-WW2 tandem module were obtained at 200-ns time intervals over a simulation time of 2μs. All 10 structures were superimposed with respect to the backbone atoms (N, Cα and C) of the core regions of WW1 (residues 22–43) and WW2 (residues 63–84) domains. In each case, the constituent WW1 (residues 22–43) and WW2 (residues 63–84) domains are respectively colored red and green, while the N-terminal loop (residues 16–21), interdomain linker (residues 44–62) and C-terminal loop (residues 85–91) are respectively shown in blue, gray and magenta. In (b), the p73 peptide is not shown for clarity. All MD simulations were performed with the GROMACS software (87) using the integrated AMBER99SB-ILDN force field (88, 89). Structural snapshots of WW1-WW2 tandem module taken at various time intervals during the course of MD simulations were superimposed using MOLMOL (90)

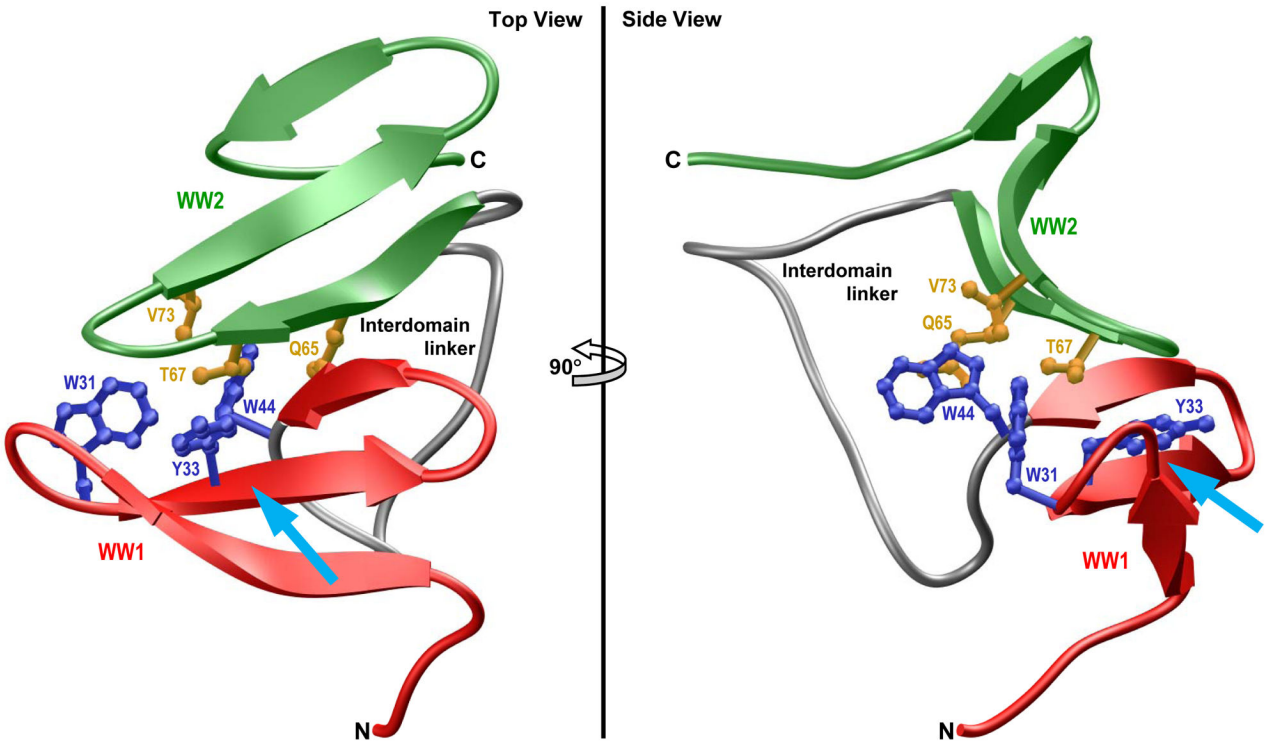

Figure 3.

Ribbon representation of the simulated structure of unliganded WW1-WW2 tandem module of WWOX obtained after 2μs of simulation time. Two alternative orientations related by a 90°-rotation about the vertical axis are depicted for closer inspection. The WW1 and WW2 domains are respectively colored red and green, while the interdomain linker is depicted in gray. Additionally, the sidechain moieties of residues within the WW1 and WW2 domains engaged in interdomain contacts are shown in blue and yellow, respectively. The cyan arrow indicates the direction of the incoming ligand as it would dock into the hydrophobic groove located on the concave face of WW1 domain, the same face that partially engages in interdomain contacts with the WW2 domain, in a competitive manner. The simulated structure of WW1-WW2 tandem module was rendered using RIBBONS (86).

```
WWOX_WW1    DELPPGWEERTTKDGWVYYANHTEEKTQWEHPKTG
ITCH_WW1    APLPPGWEQRVDQHGRVYYVDHVEKRTTWDRPEPL
ITCH_WW2    EPLPPGWERRVDNMGRIYYVDHFTRTTTWQRPTLE
ITCH_WW3    GPLPPGWEKRTDSNGRVYFVNHNTRITQWEDPRSQ
NEDD4_WW1   SPLPPGWEERQDILGRTYYVNHESRRTQWKRPTPQ
NEDD4_WW3   GFLPKGWEVRHAPNGRPFFIDHNTKTTTWEDPRLK
NEDD4_WW4   GPLPPGWEERTHTDGRIFYINHNIKRTQWEDPRLE
NEDD4L_WW2  PGLPSGWEERKDAKGRTYYVNHNNRTTTWTRPIMQ
NEDD4L_WW3  SFLPPGWEMRIAPNGRPFFIDHNTKTTTWEDPRLK
NEDD4L_WW4  GPLPPGWEERIHLDGRTFYIDHNSKITQWEDPRLQ
SUDX_WW1    EPLPAGWEIRLDQYGRRYYVDHNTRSTYWEKPTPL
SUDX_WW2    TPLPPGWEIRKDGRGRVYYVDHNTRKTTWQRPNSE
WWP1_WW1    ETLPSGWEQRKDPHGRTYYVDHNTRTTTWERPQPL
WWP1_WW2    QPLPPGWERRVDDRRRVYYVDHNTRTTTWQRPTME
WWP1_WW3    GPLPPGWEKRVDSTDRVYFVNHNTKTTQWEDPRTQ
WWP2_WW1    DALPAGWEQRELPNGRVYYVDHNTKTTTWERPLPP
WWP2_WW2    RPLPPGWEKRTDPRGRFYYVDHNTRTTTWQRPTAE
```

Figure 4.

Amino acid sequence alignment of WW1 domain of WWOX with other WW domains within the human proteome that share high sequence similarity. Note that absolutely conserved residues within the WW domains are shown in red, semi-conserved residues in blue, and all other residues are colored black.

Figure 5.

Amino acid sequence alignment of WW domains within the human proteome containing a non-tryptophan residue at the structurally-equivalent position occupied by Y85 within the WW2 domain of human WWOX. Note that the sequence alignment is sub-divided depending on whether the WW domains belong to multi-copy-WW-containing proteins (Class I) or single-copy-WW-containing proteins (Class II). The Y85 residue within the WW2 domain of WWOX and its structural-equivalents within other WW domains are colored blue. Absolutely conserved tryptophan (W63) and proline (P88), which together represent a pair of residues critical for the folding of WW domains, are shown in red. It is noteworthy that the indole and pyrrolidine sidechain rings of these conserved residues engage in stacking interactions on the convex face of WW domains, right beneath or underside of the concave ligand binding groove. In so doing, they provide a critical scaffold that is essential for the structural integrity of all WW domains.

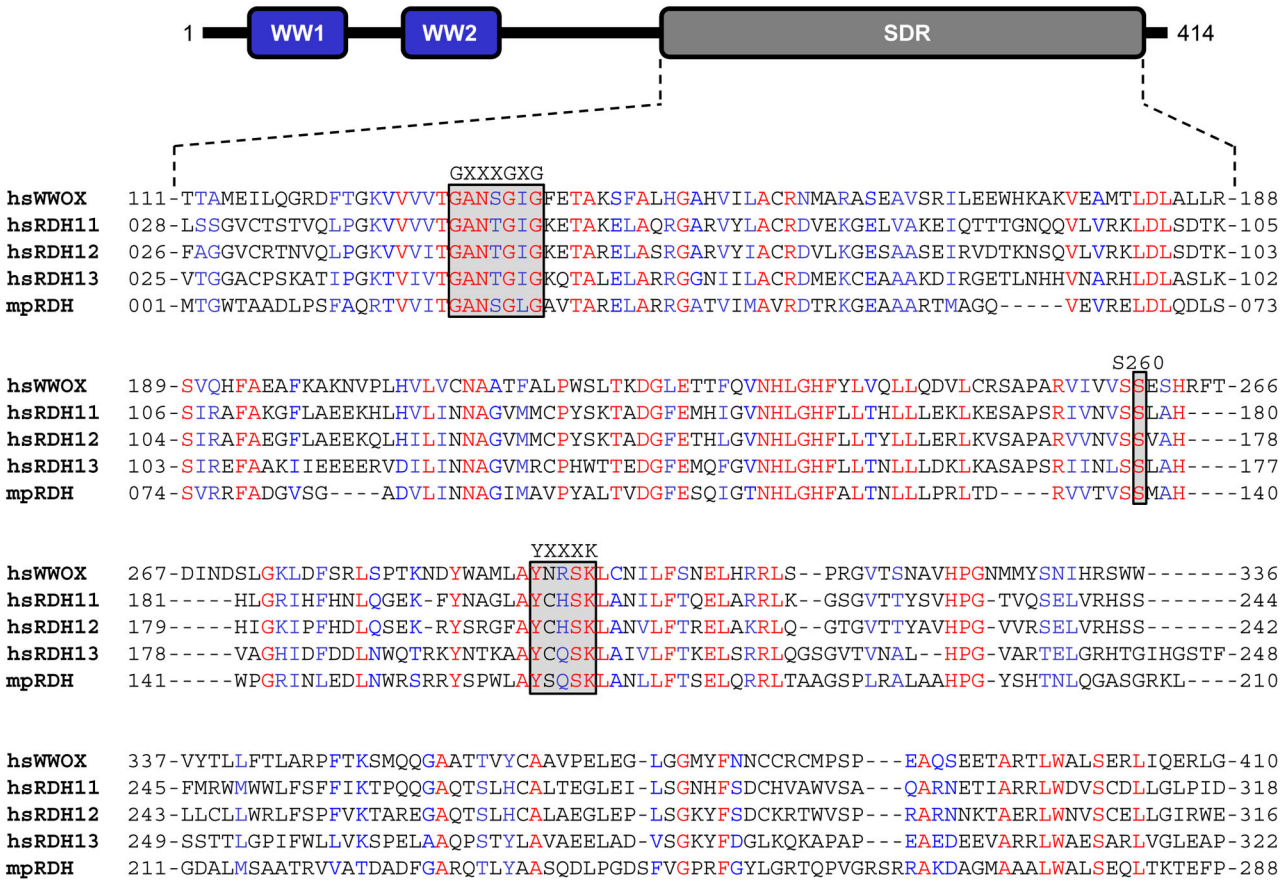

Figure 6.

Amino acid sequence alignment of SDR domains of hsWWOX (Q9NZC7), hsRDH11 (Q8TC12), hsRDH12 (Q96NR8), hsRDH13 (Q8NBN7) and mpRDH (Q741V7) derived from Homo sapiens (hs) and Mycobacterium paratuberculosis (mp). The UniProt ID of each protein is provided in the corresponding parenthesis. The numerals flanking each row of the sequence alignment denote the amino acid position of corresponding protein. Absolutely conserved residues are colored red, highly conserved residues in blue and non-conserved residues in black. The GXXXGXG motif is involved in accommodating the $NADP^+$/NADPH cofactor, while the YXXXK consensus sequence represents the active site motif critical for the enzymatic activity of SDR domains. Additionally, an absolutely conserved serine (S260 in WWOX) is required for the stabilization of retinoid substrate within the active site. Note that the modular architecture of WWOX is overlaid to indicate the relative locations of the N-terminal WW1-WW2 tandem module and the C-terminal SDR domain.

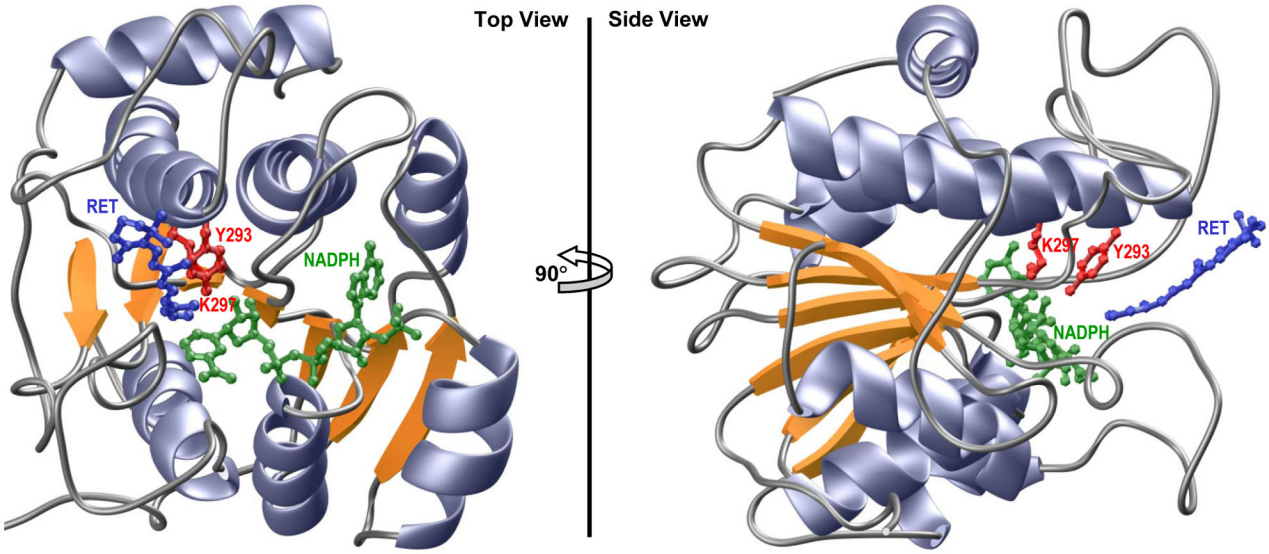

Figure 7.

Ribbon representation of the structural model of SDR domain of WWOX in complex with NADPH cofactor and all-trans-retinal (RET) substrate. Two alternative orientations related by a 90°-rotation about the vertical axis are depicted for the inquisitive eye. In each case, the β-strands are colored yellow, α-helices lavender and the intervening loops gray. The NADPH co-factor and RET substrate are shown in green and blue, respectively. The sidechain moieties of the Y293/K297 catalytic dyad, located within the RXXXK active site motif of WWOX, are depicted in red. Note that the structural model of SDR domain was built in several stages using the MODELLER software based on homology modeling (85). Firstly, the apo-structure of SDR domain was constructed using the crystal structure of mpRDH as a template (PDBID 3RD5). It should be noted here that mpRDH shares greater than 50% sequence similarity with the SDR domain of WWOX, thereby implying that the structural model of the latter can be relied upon with a high degree of confidence. Next, NADPH was mapped to the apo-structure of SDR domain on the basis of its structural homology with the crystal structure of bacterial L-sorbose reductase bound to NADPH (PDBID 3AI2). Finally, RET was docked onto the structure of SDR domain bound to NADPH in analogy with the binding mode of 17β-estradiol to 17β-hydroxysteroid dehydrogenase 1 (PDBID 1FDT) using various distance restraints between RET, NADPH and Y293 proton acceptor/donor located within the YXXXK active site motif. To ensure structural convergence, a total of 100 atomic models were calculated and the structure with the lowest energy, as judged by the MODELLER Objective Function, was selected for further analysis. The atomic models were rendered using RIBBONS (86).

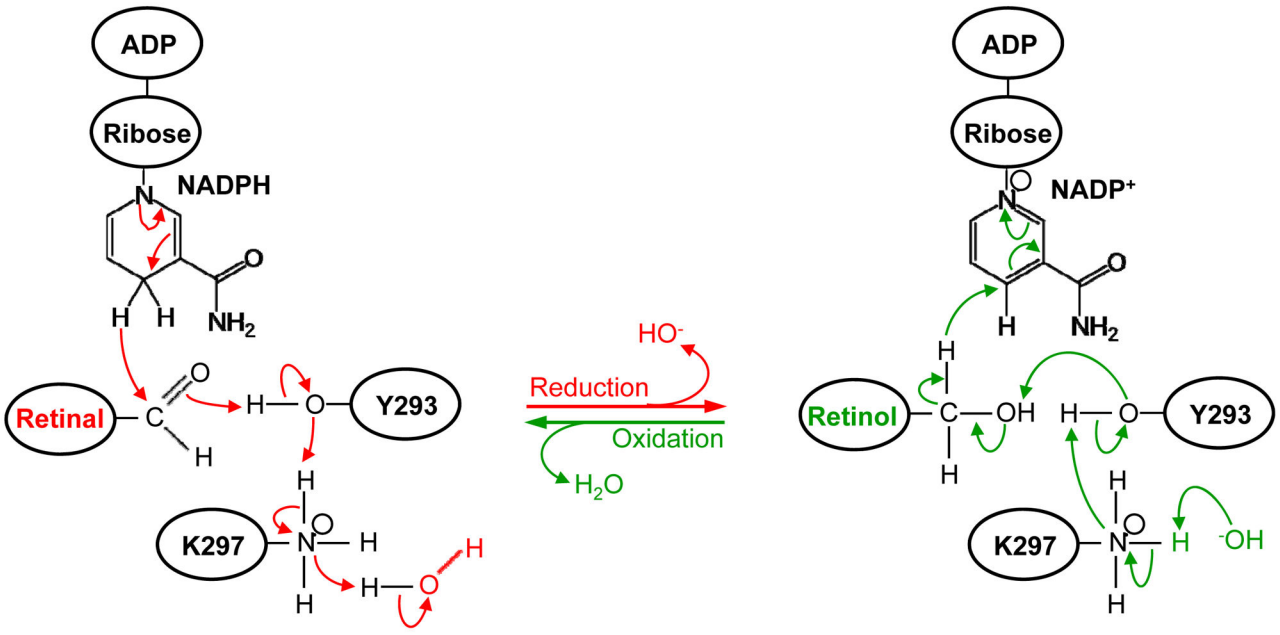

Figure 8.

A catalytic scheme proposed for the reduction and oxidation of retinal(ol) by the SDR domain of WWOX. The arrows indicate the direction of flow of a pair of electrons ($2e^-$). Additionally, both the reductive and oxidative reactions are facilitated by virtue of the ability of Y293/K297 catalytic dyad, located within the RXXXK active site motif of WWOX, to mediate acid/base catalysis.

Table 1

Comparison of the binding of WW1 domain to various PPXY-containing peptides derived from putative ligands of WWOX alone (WW1) and in the context of WW1-WW2 tandem module (WW1-WW2) in terms of the apparent equilibrium dissociation constant (K_d)

		K_d / μM	
Ligand	**Peptide Sequence**	**WW1**	**WW1-WW2**
ErbB4	TVLP**PP**P**Y**RHRN	179 ± 10	75 ± 8
p73	HCTP**PP**P**Y**HADP	107 ± 9	60 ± 6
PTCH1	RYSP**PP**P**Y**SSHS	278 ± 19	79 ± 8
PTPN14	LFRP**PP**P**Y**PRPR	763 ± 62	214 ± 30
SMAD7	LESP**PP**P**Y**SRYP	272 ± 29	53 ± 8
TMG2	HDAP**PP**P**Y**TSLR	202 ± 23	84 ± 9
WBP1	PGTP**PP**P**Y**TVAP	368 ± 44	141 ± 12
WBP2	SQPP**PP**P**Y**YPPE	133 ± 18	42 ± 7

Note that the consensus residues within the PPXY motif of each peptide are colored red for clarity. All parameters were obtained from isothermal titration calorimetry (ITC) measurements conducted at 25°C and pH 7. Errors were calculated from at least three independent measurements to one standard deviation.